

Multi-gap individual and coupled split-ring resonator structures

R. S. Penciu¹, K. Aydin², M. Kafesaki^{1,3,*}, Th. Koschny^{1,4}, E. Ozbay², E. N. Economou^{1,5},
C. M. Soukoulis^{1,3,4}

¹*Foundation for Research and Technology, Hellas (FORTH), Institute of Electronic Structure and Laser (IESL), P.O. Box 1527, 71110 Heraklion, Crete Greece*

²*Nanotechnology Research Center, Department of Physics, Department of Electrical and Electronics Engineering, Bilkent University, Bilkent, Ankara 06800, Turkey*

³*Dept. of Materials Science and Technology, University of Crete, Greece*

⁴*Department of Physics and Ames Laboratory, Iowa State University, Ames, Iowa, USA*

⁵*Physics Dept., University of Crete, Greece*

*Corresponding author kafesaki@iesl.forth.gr

Abstract: We present a systematic numerical study, validated by accompanied experimental data, of individual and coupled split ring resonators (SRRs) of a single rectangular ring with one, two and four gaps. We discuss the behavior of the magnetic resonance frequency, the magnetic field and the currents in the SRRs, as one goes from a single SRR to strongly interacting SRR pairs in the SRR plane. We show that coupling of the SRRs along the \mathbf{E} direction results to shift of the magnetic resonance frequency to lower or higher values, depending on the capacitive or inductive nature of the coupling. Strong SRR coupling along propagation direction usually results to splitting of the single SRR resonance into two distinct resonances, associated with peculiar field and current distributions.

©2008 Optical Society of America

OCIS codes: (350.3618) Left-handed materials; (350.7420) Waves

References and links

1. V. G. Veselago, "The Electrodynamics of Substances with Simultaneously Negative Values of ϵ and μ ," *Sov. Phys. Usp.* **10**, 509-514 (1968)
2. For review see at C. M. Soukoulis, M. Kafesaki, and E. N. Economou, "Negative index materials: New frontiers in optics," *Adv. Mater.* **18**, 1941-1952 (2006).
3. For review see also D. R. Smith, J. B. Pendry, and M. C. K. Wiltshire, "Metamaterials and negative refractive Index," *Science* **305**, 788-792 (2004).
4. See the special edition of *Opt. Express*: "Focus Issue: Negative Refraction and Metamaterials," *Opt. Express* **11**, 639-755 (2003).
5. R. Shelby, D. R. Smith, and S. Schultz, "Experimental verification of a negative index of refraction," *Science* **292**, 77-79 (2001).
6. R. Penciu, M. Kafesaki, T. F. Gundogdu, E. N. Economou, and C. M. Soukoulis, "Theoretical study of left-handed behavior of composite metamaterials," *Photon. Nanostruct.* **4**, 12-16 (2006).
7. T. F. Gundogdu, M. Gokkavas, K. Guven, M. Kafesaki, C. M. Soukoulis, and E. Ozbay, "Simulations and micro-fabrication of optically switchable split ring resonators," *Photon. Nanostruct.* **5**, 106-112 (2007).
8. H. Danithe, S. Foteinopoulou, and C. M. Soukoulis, "Omni-reflectance and enhanced resonant tunneling from multilayers containing left-handed materials," *Photon. Nanostruct.* **4**, 123-131 (2006).
9. N. Katsarakis, M. Kafesaki, I. Tsiapa, E. N. Economou, and C. M. Soukoulis, "High transmittance left-handed materials involving symmetric split-ring resonators," *Photon. Nanostruct.* **5**, 149-155 (2007).
10. A. J. Holden, "Towards some real applications for negative materials," *Photon. Nanostruct.* **3**, 96-99 (2005).
11. S. Guenneau, S. A. Ramakrishnan, S. Enoch, S. Chakrabarti, G. Tayeba, and B. Gralak, "Cloaking and imaging effects in plasmonic checkerboards of negative ϵ and μ and dielectric photonic crystal checkerboards," *Photon. Nanostruct.* **5**, 63-72 (2007).

12. A. Alu, N. Engheta, A. Erentok, and R. W. Ziolkowski, "Single-negative, double-negative and low index metamaterials and their electromagnetic applications," *IEEE Trans. Antennas Propag.* **49**, 23-36 (2007).
13. J. B. Pendry, A. Holden, D. Robbins, and W. Stewart, "Magnetism from Conductors and Enhanced Nonlinear Phenomena," *IEEE Trans. Microwave Theory Tech.* **47**, 2075-2084 (1999).
14. D. R. Smith, W. J. Padilla, D. C. Vier, S. C. Nemat-Nasser, and S. Schultz, "A Composite Medium with Simultaneously Negative Permeability and Permittivity," *Phys. Rev. Lett.* **84**, 4184-4187 (2000).
15. R. Marques, F. Medina, and R. Rafii-El-Idrissi, "Role of bianisotropy in negative permeability and left-handed metamaterials," *Phys. Rev. B* **65**, 144440-(1-6) (2002).
16. N. Katsarakis, T. Koschny, M. Kafesaki, E. N. Economou, and C. M. Soukoulis, "Electric Coupling to the Magnetic Resonance of Split-ring Resonators," *Appl. Phys. Lett.* **84**, 2943-2945 (2004).
17. J. Garcia-Garcia, F. Martin, J. D. Baena, R. Marques, and L. Jelinek, "On the resonances and polarizabilities of split-ring resonators," *J. Appl. Phys.* **98**, 033103-1-9 (2005).
18. T. Koschny, M. Kafesaki, E. N. Economou, and C. M. Soukoulis, "Effective Medium Theory of Left-handed Materials," *Phys. Rev. Lett.* **93**, 107402-1-4 (2004).
19. M. Kafesaki, Th. Koschny, J. Zhou, N. Katsarakis, I. Tsiapa, E. N. Economou, and C. M. Soukoulis, "Electromagnetic behavior of left-handed materials," *Physica B* **394**, 148-154 (2007).
20. K. Aydin, K. Guven, Lei Zhang, M. Kafesaki, C. M. Soukoulis, and E. Ozbay, "Experimental Observation of True Left-Handed Transmission Peaks in Metamaterials," *Opt. Lett.* **29**, 2623-2625 (2004).
21. F. Bilotti, A. Toscano, and L. Vegni, "Design of Spiral and Multiple Split-Ring Resonators for the Realization of Miniaturized Metamaterial Samples," *IEEE Trans. Antennas Propag.* **55**, 2258-2267 (2007).
22. R. Marqués, F. Mesa, J. Martel, and F. Medina, "Comparative analysis of edge- and broadside-coupled split ring resonators for metamaterial design—Theory and experiment," *IEEE Trans. Antennas Propag.* **51**, 2572-2581 (2003).
23. K. Aydin, I. Bulu, K. Guven, M. Kafesaki, C. M. Soukoulis, and E. Ozbay, "Investigation of magnetic resonances for different split-ring resonator parameters and designs," *New J. Phys.* **7**, 168-1-15 (2005).
24. M. C. K. Wiltshire, J. B. Pendry, I. R. Young, D. J. Larkman, D. J. Gilderdale, and J. V. Hajnal, "Microstructured Magnetic Materials for RF Flux Guides in Magnetic Resonance Imaging," *Science* **291**, 849 – 851 (2001).
25. V. M. Shalaev, "Optical negative-index materials," *Nature Photon.* **1**, 41-48 (2007).
26. C. M. Soukoulis, S. Linden, and M. Wegener, "Negative index metamaterials at optical wavelengths," *Science* **315**, 47-49 (2007).
27. S. Linden et al., "Photonic metamaterials: Magnetism at optical frequencies," *IEEE J. Sel. Top. Quantum Electron.* **12**, 1097-1105 (2006).
28. J. Zhou, Th. Koschny, M. Kafesaki, E. N. Economou, J. B. Pendry, and C. M. Soukoulis, "Saturation of the magnetic response of split-ring resonators at optical frequencies," *Phys. Rev. Lett.* **95**, 223902-1-4 (2005).
29. Th. Koschny, L. Zhang, and C. M. Soukoulis, "Isotropic 3d left-handed and related metamaterials," *Phys. Rev. B* **71**, 121103(R)-1-4 (2005).
30. J. D. Baena, L. Jelinek, R. Marqués, and J. Zehentner, "Electrically small isotropic three-dimensional magnetic resonators for metamaterial design," *Appl. Phys. Lett.* **88**, 134108-134110 (2006).
31. P. Gay-Balmaz and O.J.F. Martin, "Electromagnetic Resonances in Individual and Coupled Split-ring Resonators," *J. Appl. Phys.* **92**, 2929-2936 (2002).
32. J. Garcia-Garcia et al., "Miniaturized microstrip and CPW filters using coupled metamaterials resonators," *IEEE Trans. Microwave Theory Tech.* **54**, 2628-2635 (2006).
33. E. N. Economou, Th. Koschny, and C. M. Soukoulis, "Strong diamagnetic response of in split-ring-resonator metamaterials: Numerical study and two-loop model," *Phys. Rev. B* **77**, 092401-1-4 (2008).
34. S. E. Harris, J. E. Field, and A. Imamoglu, "Nonlinear optical processes using electromagnetically induced transparency," *Phys. Rev. Lett.* **64**, 1107-1110 (1990).
35. C. L. Garrido Alzar, M. A. G. Martinez, and P. Nussensveig, "Classical analog of electromagnetically induced transparency," *Am. J. Phys.* **70**, 37-41 (2002).

1. Introduction

Left-handed materials (LHMs) [1], i.e. composite materials characterized by electrical permittivity, ϵ , and magnetic permeability, μ , both negative over a common frequency band, have been a subject of impressively increased interest in the last seven years [2-9]. This is mainly due to the novel and unique properties of those materials, like backwards propagation (opposite phase and group velocities), negative refraction [4, 5], opposite radiation pressure

etc., which give them unique capabilities in the control of electromagnetic waves and the ability to revolutionized wave manipulation devices and systems [10-12].

Up to now the main approach to realize a left-handed material is to combine negative permeability with negative permittivity elements. The most common and well known negative permeability element is the split-ring resonator (SRR) structure [13], i.e. a metallic ring or concentric rings with gaps. If an alternating magnetic field is applied perpendicular to the SRR plane, the SRR behaves as a magnetic field driven inductor-capacitor (LC) circuit, exhibiting a resonant response at a frequency $\omega_m = 1/\sqrt{LC}$, associated with resonant circular currents in the ring/rings. These resonant circular currents give rise to a resonant magnetic dipole moment, thus a SRRs system can be characterized by a resonant effective permeability, which is usually followed by a negative permeability regime. One way to trace the negative permeability regime in SRRs systems is through transmission measurements or simulations, where this regime appears as a transmission dip.

Since the demonstration of the first left-handed material in 2000 [14], operating in microwaves, many studies have been devoted to the understanding of those materials [15-19], to their optimization [20-23] and to the extension of their operation frequency [24-28]. These studies resulted, among others, to design rules for SRRs appropriate for specific frequency regimes or specific applications. For example, the realization of two-dimensional and three-dimensional left-handed materials was found to require isotropic SRR designs [29, 30], free from unwanted electric field induced resonances [16, 17]; the extension of LHMs to THz and optical regimes requires simplified designs, easy to fabricate in the micro and nanometer scale, and with relatively high resonance frequency, like single ring SRRs with one or more gaps [28].

In this work we study single ring SRR designs of one, two and four gaps and we analyze the behavior of those designs, as well as the coupling between two and four SRRs in very close proximity. As it is already mentioned, those single ring designs are particularly suitable for the realization of micrometer and nanometer scale (i.e. THz and optical) left-handed materials and magnetic metamaterials, due mainly to the simplicity of the design. The presence of more than one gaps in the ring leads to an increase of the magnetic resonance frequency [23], compared to that of a single-gap ring (due to the reduced capacitance of the structure), making the two and four gap SRR even more appropriate for high frequency metamaterials. Moreover, the two and four gap structures are more isotropic, and thus free from electric resonances and other cross-polarization effects [15, 16]; thus they are appropriate for multidimensional metamaterials and metamaterials working also for unpolarized waves.

Since the realization of LHMs usually involves periodic SRR systems, it is particularly important for the design of structures targeting specific applications to understand and to be able to predict not only the behavior of a single SRR but also the coupling between neighboring SRRs. This coupling can provide an additional degree of freedom and thus an additional handle to tailor the response of SRR systems. Coupling between neighboring SRRs has been already studied for double-ring and single-ring SRRs of a single-gap [31, 32], and interesting coupling effects have been observed, like shift or splitting of the single SRR magnetic resonance frequency. Here we study this coupling for single-ring SRRs of one, two and four gaps, and in different relative orientations, resulting to a richer and more intriguing behavior.

The paper is organized as follows: In Section 2 we discuss the behavior, close to the magnetic resonance frequency, of a single SRR made of a single ring with one, two and four gaps. In Section 3 we examine the coupling when two SRRs are placed very close to each other along the incident electric field (E) direction. The SRRs are oriented in all possible mutually symmetric orientations. As we will show and explain in Section 3, the result of the coupling is in all cases a shift of the magnetic resonance frequency, which can be upwards or downwards depending on the relative orientation of the coupled SRRs. In Section 4 we

discuss the effect of the coupling when SRRs are placed very close to each other along the propagation direction. In most of the cases the effect of this coupling is a splitting of the magnetic resonance, in analogy with the splitting of two atomic states when the atoms come close to form a molecule. In Section 5 we present our conclusions.

Our model SRR is a single rectangular ring, with parameters shown in Fig. 1. The SRR is on top of a dielectric board of thickness $t_b = 1.6$ mm, and dielectric constant $\epsilon_b = 3.85$. In the coupled SRR systems the distance between neighboring SRRs is $d = 0.2$ mm (from metal edge to metal edge), while the metal conductivity in the simulations has been taken as $\sigma_m = 5.8 \times 10^7$ S/m.

All the simulations presented here have been performed using the finite integration technique (FIT), employed through the MicroWave Studio software. FIT can calculate the transmission through a finite slab excited by an electromagnetic field of a fixed polarization and constant profile, as well as to determine the fields and the currents at any point of the system, as a function of either frequency or time. In all the calculations presented here the external magnetic field is perpendicular to the SRR plane (i.e., along the z -axis - see Fig. 1(a)), while the propagation direction is in the SRR plane (in the x direction shown in Fig. 1(a)).

The experimental data shown here are free space transmission measurements obtained using a microwave Network analyzer and monopole antennas as source and receiver; the measurements procedure is identical to that described in Ref. [23].

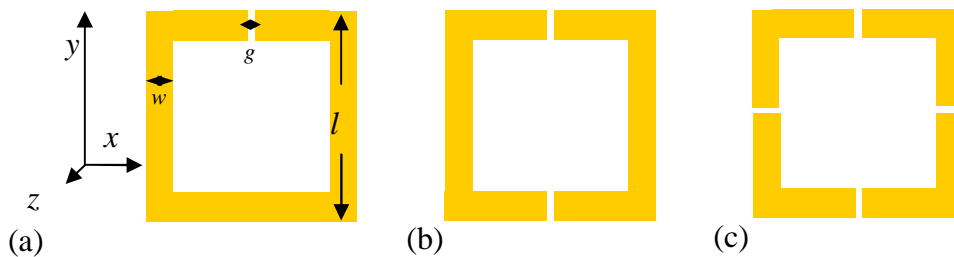


Fig. 1. The SRRs studied. Panel (a) shows the single gap SRR, where the SRR parameters are marked, panel (b) shows the two-gap SRR and panel (c) the four-gap SRR. The SRR parameters are as follows: Side length $l = 7$ mm, width of the gap/gaps $g = 0.2$ mm, metal width $w = 0.9$ mm, metal thickness $t_m = 0.03$ mm (along z -direction).

2. Individual SRRs

In this section we present and discuss the behavior of the magnetic resonance of a single SRR. This is an essential step in order to be able to analyze and understand the coupling behavior of closely placed SRRs. The single SRR behavior is studied through measurements and simulations of the transmission and reflection coefficient, as well as through simulations of the distribution of the fields and the currents at the magnetic resonance frequency.

In Fig. 2 we present the transmission (both simulated and measured) as a function of frequency for a single SRR of one gap (Fig. 2(a)), along with the surface current and the electric and magnetic fields (Fig. 2(b)) at just above the magnetic resonance frequency, ~ 3.8 GHz. From Fig. 2(a) one can see the very good agreement between theoretical and experimental data regarding the position of the magnetic resonance frequency. The difference in the transmission levels is mainly due to the difference in the measurement and simulation procedure; measurements are made in free space, with fixed in space monopole antennas as source and receiver, while for the simulation the SRR sample is essentially placed in a waveguide.

From the field and current pictures shown in Fig. 2(b) one can observe a circular current flow leading to strong magnetic field inside the SRR. This field is opposite to the incoming

magnetic field leading to the strong diamagnetic SRR response [33]. Other interesting observations are that: (a) the induced magnetic field is stronger in the regions close to the ring; (b) the main capacitive regime is the SRR gap, around which the charge concentration takes place; (c) the stronger surface current density takes place in the continuous SRR branch which is opposite to the one bearing the gap.

In Fig. 3 we show the transmission, currents and fields for a two-gap SRR, and in Fig. 4 the corresponding data for a 4-gap SRR. As expected, the resonance frequency of the two and 4-gap SRR has higher values compared to that of a single-gap SRR; the additional gaps act like capacitors in series, lowering the total capacitance of the system and increasing thus the magnetic resonance frequency, $\omega_m = 1/\sqrt{LC}$. Another interesting and unexpected observation concerns the current pictures: The total current seems to be larger at the ring parts (half-ring) which are closer to source than at the more distant parts. A possible reason for this current asymmetry may be the fact that the observed current is not only the resonant circular current excited by the external \mathbf{H} , but it is its superposition with a non-resonant current component, excited by the external \mathbf{E} , which is parallel to the sides without the gap of the ring; this superposition is addition at the ring side which is closer to the source and subtraction at the other side, contributing to the observed current asymmetry.

Comparing the transmission results of Figs. 2, 3 and 4, one can see that the higher discrepancy between theoretical and experimental data is observed for the 4-gap SRR case. We believe that this is due to the higher scattering losses in the 4-gap SRR (because of the shorter resonance wavelength - closer to the SRR size) which lead to larger deviation between simulation and experimental transmission determination procedure.

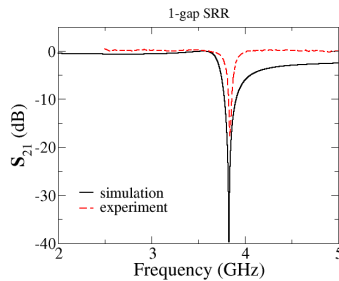


Fig. 2. (a). Transmission vs frequency for a single-gap ring. The incident electromagnetic (EM) field is as shown in Fig. 2(b). The dip around 3.8 GHz shows the magnetic resonance frequency.

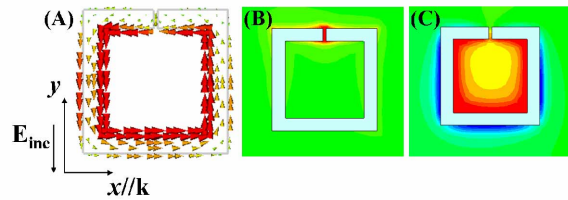


Fig. 2. (b). Current and field components at the magnetic resonance frequency for a single gap SRR. Panel (A) shows the surface current (larger arrows indicate larger current values), panel (B) shows the electric field amplitude and panel (C) the magnetic field component H_z (perpendicular to the SRR). Red color indicates large positive values (relative to the axes system shown), blue large negative values, and green small values. The propagation direction of the incident electromagnetic field is also shown in panel (A), along with the direction of the incident \mathbf{E} at the specific time point that the fields are plotted.

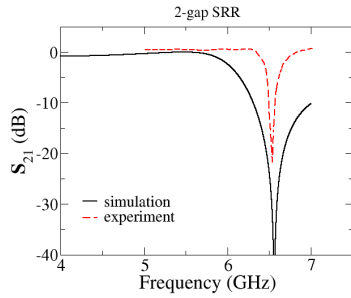


Fig. 3. (a). Transmission vs frequency for a two-gap ring. The incident EM field is as shown in Fig. 3(b). The dip around 6.6 GHz shows the magnetic resonance frequency.

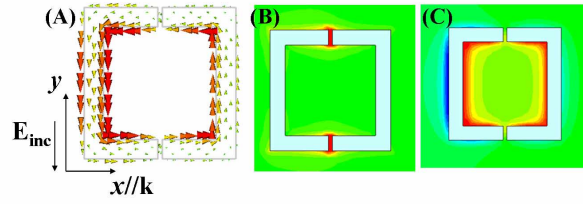


Fig. 3. (b). Current and field components at the magnetic resonance frequency for a two-gap SRR. Panel (A) shows the surface current (larger arrows indicate larger current values), panel (B) shows the electric field amplitude and panel (C) the magnetic field component H_z (perpendicular to the SRR). Red color indicates large positive values (relative to the axes system shown), blue large negative values, and green small values. The propagation direction of the incident electromagnetic field is also shown in panel (A), along with the direction of the incident \mathbf{E} at the specific time point that the fields are plotted.

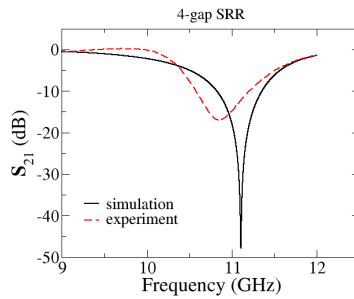


Fig. 4. (a). Transmission vs frequency for a four-gap ring. The incident EM field is as shown in Fig. 4(b). The dip around 11.1 GHz shows the magnetic resonance frequency.

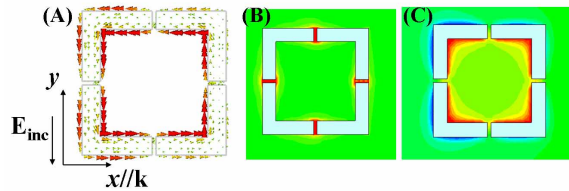


Fig. 4. (b). Current and field components at the magnetic resonance frequency for a four-gap SRR. Panel (A) shows the surface current (larger and red color arrows indicate larger current values), panel (B) shows the electric field amplitude and panel (C) the magnetic field component H_z (perpendicular to the SRR). Red color indicates large positive values (relative to the axes system shown), blue large negative values, and green small values. The propagation direction of the incident electromagnetic field is also shown in panel (A), along with the direction of the incident \mathbf{E} at the specific time point that the fields are plotted.

3. SRRs coupling along the electric field direction

In the present section we examine the coupling effects of two SRRs of one, two or four gaps. The SRRs are placed very close to each other along the external electric field direction. As we will show and explain below, the main effect of the SRRs coupling is a shift of the magnetic resonance frequency. This shift depends on the relative orientation of the interacting SRRs.

3.1. Single gap SRRs

In Fig. 5 we show the transmission as a function of frequency for a pair of closely placed SRRs (along the external electric field (\mathbf{E}) direction), in three different relative orientations, and compare these results with that of a single SRR. One can observe the quite satisfactory agreement between theoretical and experimental data (where available), taking into account that the substrate permittivity (which is extremely important in the regime between the SRRs) is not uniform in the experimental samples, and there is also an error factor in the distance of the SRRs involved.

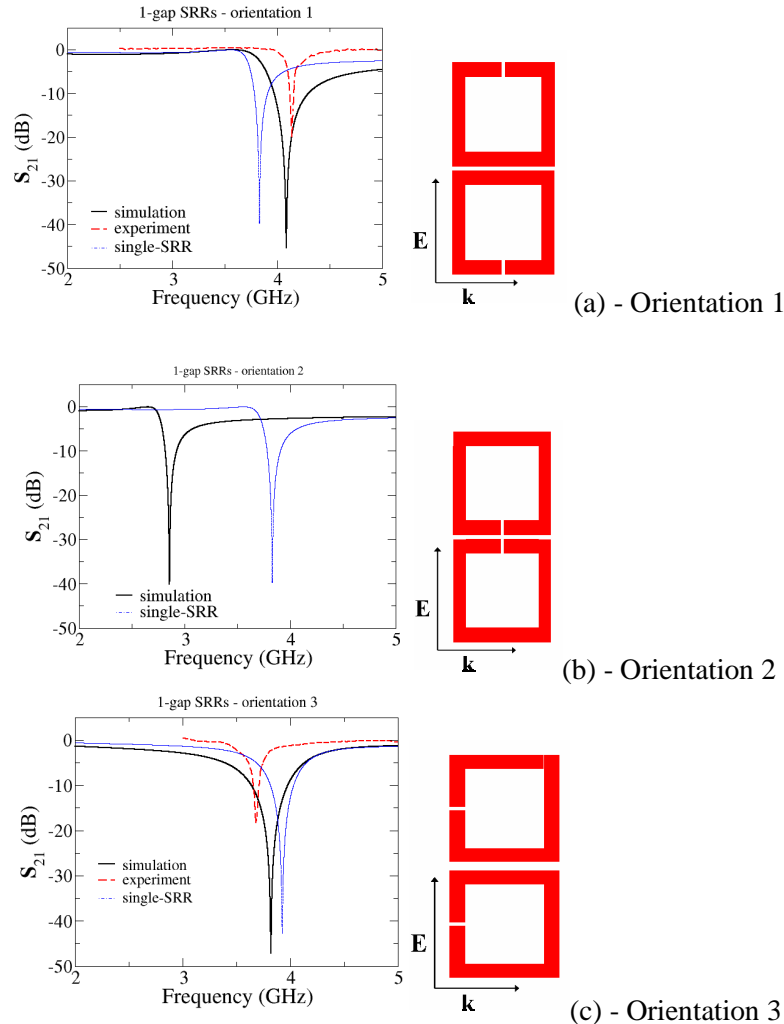


Fig. 5. Transmission vs frequency for pairs of strongly interacting SRRs, paired along the external electric field (\mathbf{E}) direction. The transmission for different relative orientations of the two SRRs in the pair is shown, marked as orientation 1 (panel (a)), 2 (panel (b)), and 3 (panel (c)). For comparison, the transmission (simulated) for a single SRR is also shown (blue, dotted-dashed line). Panels (a) and (c) show both simulation and experimental data for the pair transmission. The SRR parameters are those mentioned in Fig. 1; the SRRs distance in the pair is 0.2 mm (from metal edge to neighboring metal edge).

Examining the transmission data of Fig. 5, one can see that the interaction of the SRRs in the pair results to a shift of the magnetic resonance frequency compared to that of a single SRR (shown with the blue dotted-dashed lines in the figure) for all orientations. This shift,

while it is upwards for the orientation 1, it is downwards for the orientation 2 and very small for orientation 3.

To understand this counterintuitive difference among orientations 1-3, we examined the electric and magnetic fields, as well as the surface currents, at the resonance frequencies of the SRR couples. Figure 6 shows the electric field amplitude and the magnetic field component H_z (perpendicular to the SRRs-plane) at the magnetic resonance frequency for the orientation 1, while Fig. 7 shows the same data for the orientation 2.

As can be seen from Fig. 6, orientation 1 is associated with strong magnetic field (and negligible electric field) in the area between the SRRs, indicating strong inductive coupling between these SRRs. This is not unexpected, taken into account that the neighboring sides of the paired SRRs are the “stronger current” sides of each SRR (as was shown in the previous section). In contrast, orientation 2 (see Fig. 7), is associated with negligible magnetic field between the SRRs but with strong electric field, indicating a capacitive coupling between the SRRs of the pair. This is again not surprising, as the neighboring sides of the paired SRRs are regimes of strong charge concentration, due to the presence of the gaps, and the excitation field is such that opposite charges are accumulated at the neighboring sides of those SRRs.

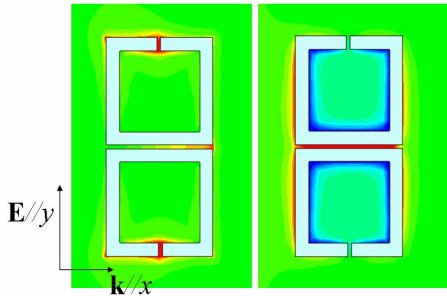


Fig. 6. The electric field amplitude $|E|$ (left) and the magnetic field component H_z (right), at the magnetic resonance frequency, for a pair of single-gap SRRs in orientation 1. Red color indicates large positive values and blue color large negative values (i.e. of field direction opposite to the axes shown). The polarization and the propagation direction of the incident field are also shown. Left panel shows that the electric field intensity is higher in the regime close to the SRR gaps; right panel indicates the excitation of circular currents of the same direction in both rings and the presence of high magnetic field in the regime between the SRRs.

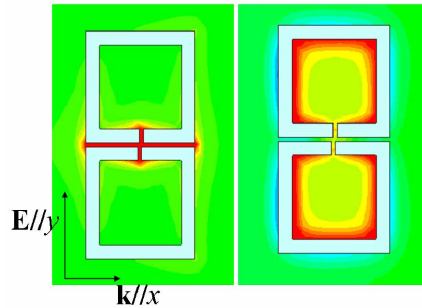


Fig. 7. The electric field amplitude $|E|$ (left) and the magnetic field component H_z (right), at the magnetic resonance frequency, for a pair of single-gap SRRs in orientation 2. Red color indicates large positive values and blue color large negative values for the magnetic field. The polarization and the propagation direction of the incident field are also shown. Left panel shows that higher electric field intensity occurs in the SRR gaps and in the regime between the two SRRs; right panel indicates the excitation of circular currents of the same direction in both rings and the presence of negligible magnetic field in the regime between the rings.

The above observations can easily explain the different direction of the magnetic resonance shift for the orientations 1 and 2: Inductive coupling introduces a mutual inductance in the system, L_{mut} , in parallel to the self-inductance of each SRR, L . L_{mut} results to a lowering of the total inductance of the SRR ($1/L_{tot}=1/L+1/L_{mut}$), and thus to an increase of the resonance frequency. (An alternative way to describe this is by noticing that the flux, Φ , ($\Phi =LI$), at each SRR reduces the flux of its neighboring ring, resulting to a lower “effective” inductance.) This seems to be the case whenever the neighboring sides of the paired-SRRs are regions of strong currents. In contrast, when the neighboring SRRs sides are regimes of strong charge accumulation, the main contribution to the coupling is through the capacitance developed between the SRRs, C_{mut} , in parallel with the

individual rings capacitance, C . This additional capacitance results to increase of the total capacitance of the system ($C_{\text{tot}}=C+C_{\text{mut}}$) and thus to decrease of the magnetic resonance frequency. This seems to be always the case when the neighboring sides of the paired rings are regimes of strong charge concentration, i.e. gap bearing sides. The above observations will be confirmed further from the study of two-gap and four-gap SRRs.

Observing the fields and currents for orientation 3 (not shown here), where the neighboring sides of the paired SRRs are neither strong currents nor charge concentration regimes, we see that orientation 3 is associated with weak coupling, both capacitive and inductive. The weaker coupling and the interplay of the upwards shift originated from the inductive interaction with the downwards shift due to the capacity interactions results to an insignificant shift of the resonance frequency of the pair compared to that of a single SRR, as is shown in Fig. 5(c).

3.2. Two gap SRRs

In Fig. 8 we show the transmission vs frequency for a pair of strongly interacting two-gap SRRs in the two possible relative (mutually symmetric) orientations.

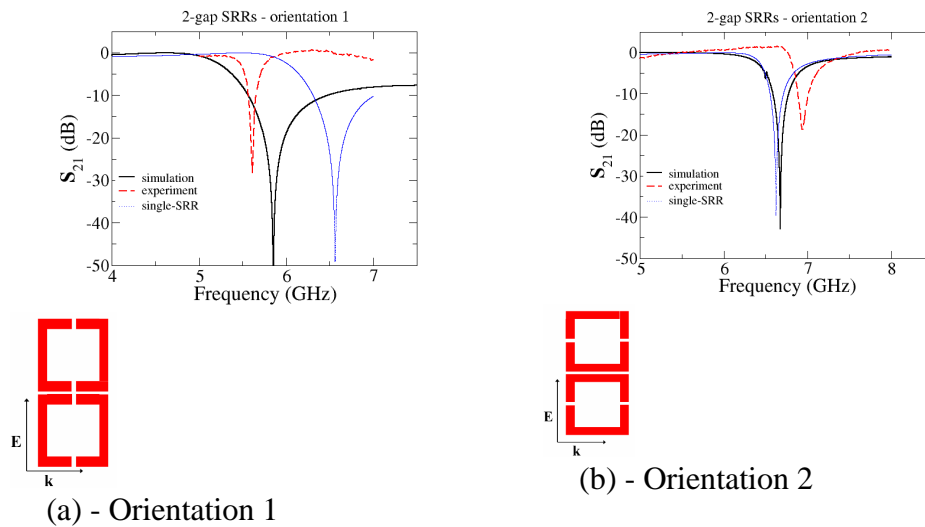


Fig. 8. Electromagnetic wave transmission vs frequency for a pair of strongly interacting two-gap SRRs in two relative orientations. For comparison, the transmission (simulated) for a single SRR is also shown (blue-dotted line).

As can be seen in Fig. 8, coupling through orientation 1 has as a result the lowering of the magnetic resonance frequency of the pair compared to that of a single SRR, while orientation 2 results to a slight upwards shift of that frequency. Examining the fields and the currents in both cases we can see that the coupling in the case of orientation 1 is mainly capacitive, leading thus to a downwards shift of the magnetic resonance, as was discussed in the previous subsection. This is in agreement also with the conclusion (see previous subsection) that gap-bearing neighboring sides (along with symmetric excitation in the two SRRs) result to capacitive coupling. For the orientation 2, observation of fields and currents shows that the coupling is both capacitive and inductive. The slight upwards shift of the magnetic resonance in this case indicates a slightly larger role of the inductive coupling.

3.3 Four gap SRRs

Here we discuss the coupling effects for SRRs of four gaps. In the case of 4-gap SRRs and for incidence in the plane of the SRRs, there is a unique possible relative orientation of the rings,

as shown in Fig. 9. Due to the fact that the neighboring sides of the paired-SRRs in this case are gap-bearing sides, i.e. regimes of strong charge concentration, one expects mainly capacitive coupling between the rings, i.e. downwards shift of the single SRR magnetic resonance frequency. This is confirmed from the transmission spectra of Fig. 9, as well as from the fields and currents pictures at the magnetic resonance (not shown here).

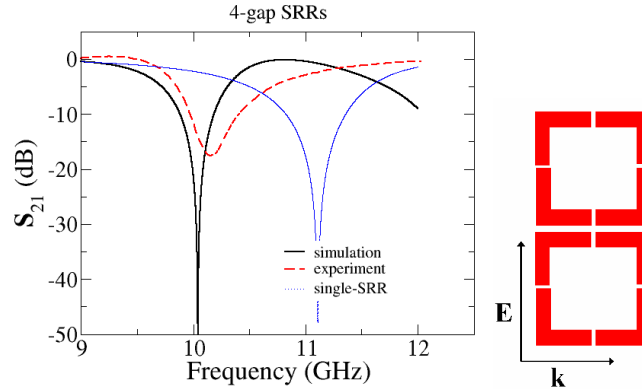


Fig. 9. Electromagnetic wave transmission vs frequency for a pair of strongly interacting 4-gap SRRs. Solid-black line shows the simulations data and dashed-red the corresponding experimental ones. For comparison the transmission (simulated) for a single SRR is also shown (dotted-blue line).

4. SRRs coupling along propagation direction

In the present section we examine the coupling effects of SRRs of one, two or four gaps are placed very close to each other along the propagation direction. Similar studies on double ring SRRs [31] showed that coupling along propagation direction results in broadening and small downwards shifting of the negative permeability regime. For very closely placed (strongly interacting) SRRs it has been observed also splitting of the magnetic resonance into two resonances.

Here, to be close to the behavior of realistic systems of many SRRs, we examine the effects of the coupling along propagation direction combined with the effects discussed in the previous section, i.e. we discuss SRRs paired along propagation direction and along electric field direction simultaneously, i.e. 2x2 SRR arrangements.

4.1. Single gap SRRs

In Fig. 10 we show the transmission vs. frequency for a single-gap SRRs pair, as those discussed in the previous section, coupled with a second identical pair along propagation direction, in four different relative orientations of the two pairs. For comparison, the transmission for only one pair is shown, copied from Fig. 5. Note that orientations 1 and 2 of Fig. 5 give one configuration possibility (each) in the 2x2 set, while orientation 3 gives two possibilities, marked as orientation 3a and 3b in Fig. 10.

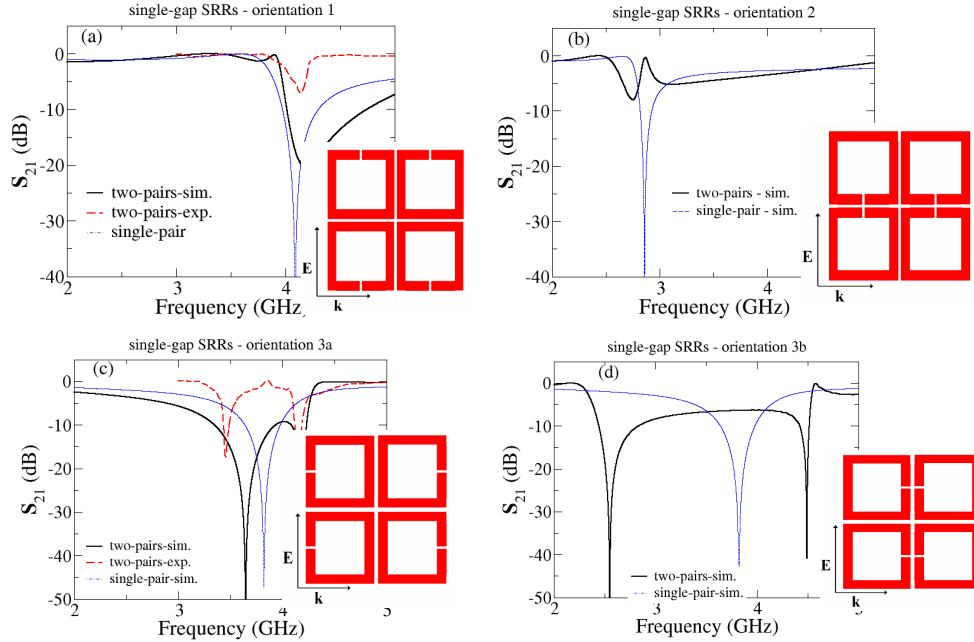


Fig. 10. Transmission vs. frequency if two pairs of single-gap SRRs, like those of Fig. 5, are placed next to each other along propagation direction (distance between pairs is 0.2 mm – from metal edge to metal edge). Solid-black lines show simulation results and dashed-red lines experimental data (where available). For comparison, the simulated transmission for a single pair is shown (blue-dotted-dashed lines).

It is worth-noticing in Fig. 10 the difference in the coupling effects between orientations 1 and 2 on one hand and orientations 3 on the other. In orientations 3 the addition of a second pair along propagation direction results to a clear splitting of the magnetic resonance into two resonances, while in orientations 1 and 2 the coupling of the two pairs seems to result to a weakening and possibly broadening of the magnetic resonance. A detailed investigation though reveals two resonances also for orientations 1 and 2, but much weaker and close to each other. A possible explanation of this difference can come from the fact that the coupling in orientations 1 and 2 is through the SRR sides which are of weak current and weak charge concentration; this may result to a weak coupling. In addition, the simultaneous capacitive and inductive nature of this coupling, counteracting each other, leads to not clear effects. In orientations 3, in contrast, the coupling is through sides of either strong current (orientation 3a), i.e. strong inductive interaction, or of strong charge concentration (orientation 3b), i.e. strong capacitive coupling.

To understand further the origin of the different coupling effects between orientations 1 and 2 on one hand and orientations 3 on the other, as well as between the two different possibilities of orientation 3, we examined the fields and the currents at the different resonance frequencies. In Fig. 11 we plot the perpendicular to the SRRs component of the magnetic field at the resonance frequency, for all the resonance frequencies appearing in Fig. 10.

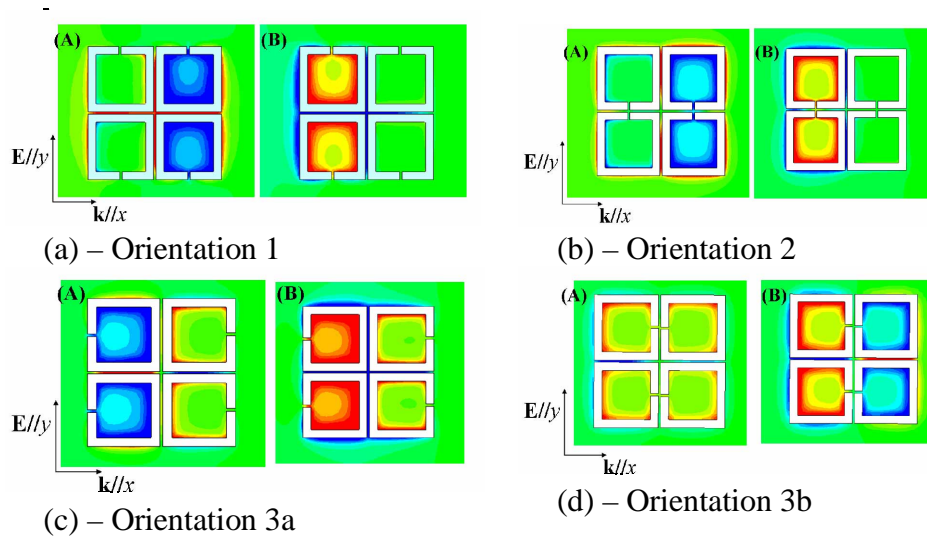


Fig. 11. The magnetic field component H_z at the different magnetic resonance frequencies appearing in Fig. 10. (a): Orientation 1, shown in Fig. 10(a). Panel (A) shows the first resonance, at 3.8 GHz, panel (B) the second resonance, at 4.2 GHz. (b): Orientation 2, shown in Fig. 10(b). Panel (A) shows the first resonance, at 2.71 GHz, panel (B) the second resonance, at 3 GHz. (c): Orientation 3a, shown in Fig. 10(c). Panel (A) shows the first resonance, at 3.65 GHz, panel (B) the second resonance, at 4.2 GHz. (d): Orientation 3b, shown in Fig. 10(d). Panel (A) shows the first resonance, at 2.5 GHz, panel (B) the second resonance, at 4.5 GHz. Red color indicates large positive values, blue color large negative values, green color small values. The external wave incidents always from left-side of the system.

What we observed from the fields and currents distribution is that in the resonances of orientation 1 and 2 only one of the pairs is excited, while the other remains silent. In some cases the pair which is away from the source seems to be excited, while the closer to the source one seems almost completely inactive. To understand the selective excitation of only one pair of rings we must take into account that because of the symmetry of the structure, the coupling of the two pairs leads to two “eigenmodes” one of even and the other of odd symmetry, i.e. one with same direction currents in both pairs and one with opposite direction currents. A field which is symmetric with respect of the two pairs will excite the symmetric mode and an antisymmetric external field will excite the antisymmetric one. In both cases the two pairs will be equally excited. If the excitation field is neither symmetric nor antisymmetric (e.g. if the two pairs see fields differing neither by zero nor by 180 degrees) the excitation of the two pairs will be unequal and it is quite possible, depending on the equality of the field amplitudes of the even and odd modes and the phase difference of the external field between the two pairs, to silence any one of the two pairs. This silencing is more frequent in the case where the eigenfrequencies of the even and odd eigenmodes are close together, as in the case of orientations 1 and 2, and the phase difference is quite substantial. In contrast, for orientations 3, where the two resonances are well separated in frequency, either the even or the odd symmetry is predominantly excited resonantly, while the other eigenmode is almost inactive. As a result one of the resonant excitations leads to circular currents of the same direction in both pairs and the other one to opposite direction currents.

Concerning orientations 3a and 3b, there are some additional worth noticing features and differences: (a) In both cases we observe splitting of the single-pair magnetic resonance into two resonances; in orientation 3a though the splitting is smaller than that in 3b. (b) The lower resonance in orientation 3a is associated with currents of opposite direction in both pairs and the upper resonance with currents of the same direction. The opposite happens in the case of

orientation 3b: lower resonance is associated with currents of the same direction in both pairs and higher resonances with currents of opposite direction.

Both features can be explained by taking into account that the coupling of the two pairs is mainly inductive in orientation 3a (since branches of strong current are close to each other) and capacitive in 3b. The first feature is explained by the fact that the capacitive coupling is electrostatic in nature and, hence, stronger than the inductive, which is magnetic and, hence, weaker. The second feature can be understood by analyzing more the effect of parallel and antiparallel currents in orientations 3a and 3b: In orientation 3a currents of the same direction result to decrease of the flux, $\Phi=LI$, at each pair due to the presence of its neighbor, i.e. decrease of the effective inductance and thus increase of the magnetic resonance frequency. For the same reason, currents of opposite direction result to lowering of the resonance frequency. Thus the lower frequency is associated with opposite direction currents and the higher with currents of the same direction. In orientation 3b, in contrast, there is not large flux from first pair penetrating to the second. There, parallel currents in the two pairs lead to opposite charges in the neighboring sides of the pairs, and thus to development of an additional capacitance, which increases the total capacitance of the system, reducing the magnetic resonance frequency. That's why for orientation 3b the lower resonance frequency corresponds to parallel currents.

4.2. Two and four gap SRRs

Repeating the investigations described in the previous subsection for SRRs of two and four gaps, we obtain the transmission pictures presented in Fig. 12.

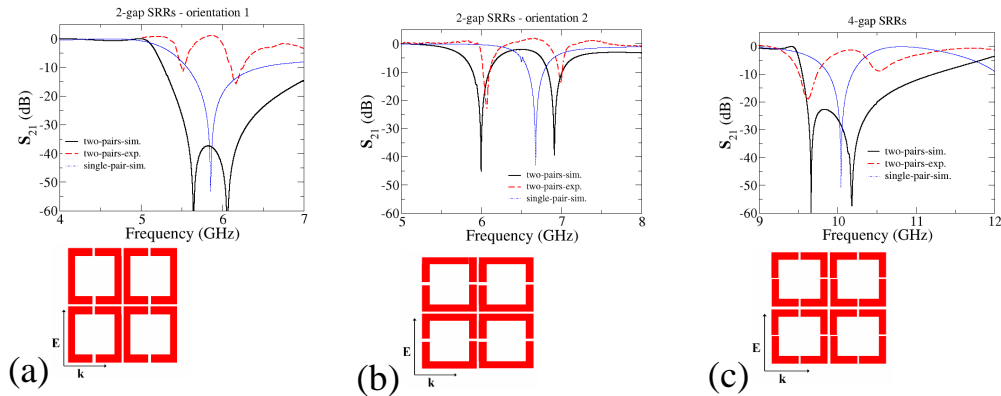


Fig. 12. Panels (a) and (b): Transmission vs. frequency if two pairs of two-gap SRRs, like those discussed in Fig. 8, are placed next to each other along propagation direction (distance between pairs is 0.2 mm – from metal edge to metal edge). Solid-black lines show simulation results and dashed-red lines experimental data. For comparison, the simulated transmission for a single pair is shown (blue-dotted-dashed lines). Panel (c) shows the same data as panels (a) and (b) for 4-gap SRRs.

In all cases we observe splitting of the magnetic resonance of a single pair (see blue-dotted-dashed lines) into two distinct dips, due to the interaction of the two pairs along propagation direction. The splitting is small for orientation 1 of the two-gap case, since the interacting sides of the pairs are not regions of either strong currents (i.e. not considerable inductive coupling) or strong charge concentration (i.e. not considerable capacitive coupling), and larger for orientation 2, where strong capacitive coupling takes place, as is revealed also from the examination of fields at the resonances (not shown here). Examination of those fields and currents shows also that, like in the case of Fig. 11 (see panel (d)), lower resonance is associated with same direction currents in the two pairs and higher resonance with opposite direction currents.

The four gap case shown in Fig. 12(c) is rather unusual in the sense that the first resonant excitation is associated with appreciable amplitude in the second pair (away from the source) and much less in the first. This is surprising given the fact that the two eigenfrequencies (resonant frequencies) are not so close; on the other hand, the resonance of the high frequency eigenmode is rather wide and, hence, it may be excited appreciably even by external source of frequency at the low resonance. Moreover, because of the elevated frequencies of the four gap SRRs, the phase difference of the excitation field that the two pairs see is close to 90° , favoring strong mixture of the even and the odd symmetry resonant modes, leading thus to selective excitations of predominantly of one pair. This interpretation is supported by the fact that, when the external field frequency is at the higher resonance frequency, the expected behavior is observed, i.e., the odd mode is excited of about equal amplitudes in the first and the second pair. This is in accordance to our interpretation, since the low frequency resonance is quite sharp and, hence, cannot be excited appreciably by an external source of frequency coinciding with that of the higher resonance.

5. Conclusions

Using both numerical simulations and experimental measurements, we have studied single-ring SRR structures with one, two and four gaps. We focused mainly on the coupling effects of the two SRRs when they are placed in close proximity along propagation direction and along the external electric field, \mathbf{E} , direction.

We found that coupling along the external \mathbf{E} direction results to shift of the magnetic resonance frequency of the single SRR; the shift is upwards when the neighboring sides of the coupled SRRs are regimes of strong currents and downwards when the neighboring sides are regimes of strong charge concentration. The upwards shift in the first case is due to an inductive interaction of the SRRs, resulting to a reduction of the effective inductance of each SRR; the downwards shift in the second case is due to a capacitive interaction between the SRRs, resulting to additional capacitance in the system.

Concerning the coupling along propagation direction, we found that in most of the cases this coupling results to splitting of the magnetic resonance into two distinct resonances; the field and current distribution at those resonances can be explained taking into account the capacitive or inductive nature of the coupling. In the case of two pairs in close proximity along the propagation direction, a very interesting effect appears under certain conditions: One of the two pairs may be partially or fully silenced, while the other is fully excited, in spite of the external field frequency being equal to one of the two eigenfrequencies. For this effect to occur the two eigenfrequencies have to be close to each other (relative to their width) and an appropriate phase difference of the external field between the two pairs along the propagation direction must appear. This phenomenon is the SRRs analog of the electromagnetically induced transparency (EIT) [34], according to which one of the two atomic transitions is silenced under appropriate conditions (see also [34]).

Acknowledgments

Authors would like to acknowledge financial support by EU under the projects Metamorphose, PHOREMOST, Molecular Imaging (LSHG-CT-2003-503259), PHOME (FET Contract No. 213390) and ENSEMBLE, by the US Department of Energy (Basic Energy Sciences) under Contract No. DE-AC02-07CH11358, by the AFOSR under MURI grant (FA9550-06-1-0337), by DARPA (Contract No. MDA-972-01-2-0016), by Office of Naval Research (Award No. N00014-07-1-0359).